Assiut Univ. J. of Physics **Printed ISSN 1687-4900**
49(2), pp.35-49 (2020)

FTIR SPECTROSCOPY STUDY ON THE IMPACT OF LOW POWER NEAR-INFRARED LASER ON THE SECONDARY STRUCTURE OF HUMAN HEMOGLOBIN (IN-VITRO)

M. Bysam[1,*], A. Sedky[1], Wael M Elshemey [2], and Haitham S. Mohammed[2]

[1] Physics Department, Faculty of Science, Assiut University,71516 Assiut, Egypt
[2]Biophysics Department, Faculty of Science, Cairo University 12613, Giza, Egypt

Received: 25/8/2020 **Accepted:** 29/9/2020 **Available Online:** 1/12/2020

The low-level laser therapy was used in various biomedical applications for a long time such as improving the rheological properties of blood, wound healing, vascular restenosis, tissue repair. however, its safety has not been well investigated. The present in-vitro study aims to illustrate the influence of low power laser irradiation on the secondary structure of human Haemoglobin (Hb). Fifteen samples of healthy fresh blood have been divided into five groups (3 samples/group) and irradiated using low power infrared laser (wavelength 808 nm, power 4 mw and power density 0.64 mW/cm^2) at different irradiation durations (5, 10, 20, 30 min) and zero time for control samples. We used FTIR Spectroscopy followed by some mathematical techniques such as band-narrowing (second-derivative method), spectral subtraction, curve fitting, and integration processes to quantitatively calculate the different contribution ratios of the secondary structure components of irradiated and non-irradiated human hemoglobin samples. It was found no significant change in the contents of the α-helix structure at (5,10,20 min) groups. However, the thirty minutes group (30min) show a significant reduction in the content of α -helix accompanied by a significant increase in the random coil and β-turn structures with ($p < 0.05$). The decreasing of the alpha-helix structure is explained in terms of photo-inductive degradation to the unordered structure of random coils and β-turns. Extra care has to be taken while the clinical application that includes the intravenous laser irradiation of blood to avoid the protein photodamage caused by the low power laser at long expoture time.

Keywords: Hemoglobin; Secondary structures; FTIR; Low power laser
*Corresponding author: Tel.: +201002974733
E-mail.: bysem@yahoo.com

1. INTRODUCTION

Lasers are devices that produce polarized and relatively coherent electromagnetic radiations, investigated for the first time in 1960 by T.Maiman [1]. Since this year and till now, the previous unusual properties of the laser have been led it to be used in a wide range of clinical procedures such as dermatology, surgery, activating the photodynamic agents, wound healings, and ablative treatments that depend on the generation of heat by the laser beam such as in cosmetic surgery. Lasers that are used for high energy medical applications such as the ablative treatments, cutting and thermal

coagulating of tissues are required a high power range (10:100 Watts) [2].on the other hand, Lasers that have a low power range (1:500 mW) are known as low-level laser which widely used in the photochemical reactions such as the Photodynamic therapy and Biostimulation [2,3]. The term "Biostimulation" also recognized as Photobiomodulation was originally described by the Hungarian surgeon Endre Mester in 1967. It was defined as the application of low power laser on biological system to induce tissue regeneration such as happen in the wound healing clinical procedure by laser. Mester experimented in order to study the impact of laser irradiation on the hair growth of mice and tested if it might cause cancer or not and observed, that the hair of the irradiated mice grew back faster than the non-irradiated [4]. Low power laser therapy does not have any thermal or ablative mechanisms, but only have a photochemical influence which indicates that the low power laser irradiation is absorbed by molecular absorption bands of some photo-sensitive molecules known as "chromophores" causing a chemical change [3,5].

The effective tissue penetration of light (optical window) has a maximum value range from 650 nm to 1200 nm. The blue region has a higher rate of scattering and absorption in tissues than the red region, this can be attributed to the efficient absorption ability of hemoglobin and melanin, which are the major tissue chromophores[6]. hemoglobin has very high absorption bands at wavelengths lower than 600 nm, light scattering coefficient of tissues is higher at shorter wavelengths, also water intensely absorbs infrared light at wavelengths higher than 1100 nm. Therefore the use of low power laser in biological systems approximately includes this range (600-1100 nm)[7]. The therapeutic effect and cellular scale biological mechanisms of low power laser irradiations at different wavelengths and different light doses in the biomedical field are well known. These include wound healing, vascular restenosis, tissue repair, and improving the erythrocyte deformability [8,9]. In China, the clinical procedures that include intravenous low power laser irradiation such as the treatment of psoriasis, cerebral infarction, and rheumatoid arthritis are applied and the results were positive and encouraging, However, the biochemical interaction mechanism of laser light with living cells is not totally understood[2-7]. On the other hand, previous Raman spectroscopy studies on the impact of low-level laser irradiation on red blood cells and hemoglobin have shown significant photo-induced damage for long irradiation durations[14–16].

Hemoglobin (Hb) is the most dominant protein in the blood. It has a globular quaternary structure and is the oxygen-transporter metalloprotein in erythrocytes of almost all vertebrates. The environmental changes such as temperature increase, pH fluctuations, and chemical modifications can cause structural alterations in Hb molecules which affect its function [17]. The

most common techniques used for describing the three-dimensional structure of proteins are X-ray crystallography and NMR. Nevertheless, X-ray crystallography requires a crystal structure of proteins which is challenging for almost of proteins. The NMR structure spectra of proteins can be determined in solution however, it is limited to low-weight proteins. Those previous limitations to structure generation at the atomic resolution have led to the development of alternative methods that can provide molecular structural information of proteins such as Fourier transform infrared (FTIR) spectroscopy, circular dichroism (CD), and Raman spectroscopy. Circular dichroism is cconsidered as the most common technique used for calculating the secondary structure components of proteins However, it is limited to only optically clear solutions [13,14].

In the last decade, the mathematical techniques such as band-narrowing (Second-derivative and Fourier self-deconvolution techniques), spectral subtraction, and curve fitting have led to a considerable expansion in the using of FTIR spectroscopy to estimate the contribution of secondary structure components quantitively. Fourier transform infrared (FTIR) spectroscopy represents a measurement of wavenumber vs intensity of the transmittance of IR radiation by a sample. It is recognized as a valuable tool for determining the contents of the secondary structures of proteins in hydrated films, aqueous solution, solids, organic solvents, detergents, micelles, and phospholipid membranes. It has the advantages of being non-destructive and not limited by protein size [13-15].

This work aims to explore the influence of low-level laser irradiation on the molecular structure of Hemoglobin using IR spectroscopy, the human blood samples irradiated by an infrared laser of wavelength 808nm and power density 0.64 mW/cm^2. We used FTIR Spectroscopy followed by second derivative analysis technique, curve fitting, and integration processes to investigate the change in the molecular structure of all Hb sample groups.

2. MATERIALS AND METHODS

Laser irradiation

15 ml of healthy fresh human blood were collected through venipuncture into Ethylenediaminetetraacetic acid (EDTA) as an anticoagulant and divided into 5 groups according to the irradiation duration. Each group was composed of three samples, and each sample was about 1mL of whole blood placed in a Petri dish with a diameter of 2.5cm. The depth of the blood sample was about 0.5 mm. Low power infrared laser radiation (808 nm, and energy density of 0.64 W/cm^2) was used to irradiate the samples for different durations (5, 10, 20, 30 min and zero time for the control samples).

Hb sample preparation

After irradiation, the samples of whole blood were centrifuged at 2000 rpm(revolution per minute) for 10 min, and the clear plasma was discarded. The packed red blood cells (RBCs) were cleaned three times with 0.9% NaCl (10 ml per ml of packed RBCs) and centrifuged at 3500 rpm for 5 min; the supernatant was discarded. To eliminate the impact of the RBCs membrane and evaluate the impact of low power laser on Hb, the packed RBCs were lysed by adding-ionized water with a volumetric ratio of 1:10, then centrifuged at (12,000 rpm for 45 min at 4 °C). The supernatants were carefully separated and Freeze-dried to remove water from Hb samples for FTIR spectroscopy measurements.

FTIR measurements

Hemoglobin spectra were recorded using Nicolet 6700 Thermo scientific spectrometer. The freeze-dried Hb samples were mixed with dried KBr at a ratio of 1:100, and pellets were prepared for measurements. The spectra of the 15 samples were generally collected using a 4 cm^{-1} resolution. Every sample had an average of 16 scans where the overlapping spectra of water vapor and air were filed as background and subtracted iteratively until a straight baseline is established in the range of (2000 – 1750) cm^{-1} of FTIR spectra as shown in fig1. The data obtained was smoothed and normalized using origin 8 software.

3. Mathematical background

The Secondary structure of proteins refers to the array of amino acid residues in a polypeptide chain and is mainly composed of α-helices, β-sheets, β-turns, and random coils. The alteration of the secondary structure of proteins is referred as a change in the ratios of those common structure types. The FTIR bands of proteins are usually interpreted in terms of the vibrations of a structural repeat unit which gives up to 9 essential bands referred as amide A, B, I, II ... VII. Those distinctive FTIR bands of proteins are presented in Fig 1. the Amids A and B at 3300 cm^{-1} and 3100 cm^{-1} respectively are mainly formed from N-H stretching. While the amide III which located at 1229−1301 cm^{-1} is associated to C-N stretching and N-H bending. Amid IV,V,VI at 625−767 cm^{-1}, 640−800 cm^{-1}, 537−606 cm^{-1} is attributed to O-C-N bending, N-H bending and C=O bending respectively [13,14].

Amide I and amide II bands are the two major bands associated with the secondary structure of the protein infrared spectrum. The amide I band that in the range of (1600 - 1700 cm^{-1}) has the strongest response to any conformational change because it mainly resulting from the C=O stretching

vibration (70-85%) coupled with N-H bending of the and C-N stretching (15-30%). Amide II is assigned to the N-H bending (40-60%) and the C-N stretching vibration (18-40%). The other amide bands are difficult to use in molecular structure estimation because of their complexity [13-15].

The computerized FTIR instrumentation followed by band narrowing techniques such as second derivative analysis and Fourier Self-Deconvolution (FSD) provided the basis for the quantitative estimation of protein secondary structure. The quantitative analysis relies on the idea that proteins can be treated as a linear summation of the major secondary structural components. In the amide I region (1700−1600 cm^{-1}) every different conformotion of the secondary structure has its own characteristic C=O stretching frequency due to distinctive molecular geometry and hydrogen-bonding pattern. Amide I absorbance is usually a single broadband. Therefore, baseline correction, band-narrowing method (second derivative analysis), and curve fitting are required to resolve the interfering bands. The basic idea of the second derivative analysis method is that the intrinsic shape of an infrared band absorbance of spectrum $A(\nu)$ can approximated by a following Lorentzian function ;

$$A(\nu) = \frac{A_0 \gamma^2}{\gamma^2 + (\nu - \nu_0)^2} \qquad (1)$$

Where ν is the wavenumber (in units of cm^{-1}), A_0 is the maximum absorbance of the band corresponding to wavenumber ν_0 and γ is half-width at half-height of the original spectrum. On the other hand, Fourier transform $I(x)$ of the spectrum which is a function of $A(\nu)$ is given by;

$$I(x) = F\{A(\nu)\} = \int_0^\infty A(\nu)\cos(2\pi\nu x)\,dx$$
$$= \frac{1}{2} A_0 \gamma \cos(2\pi\nu_0 x)\, e^{-2\pi\gamma x} \qquad (2)$$

Wheres x is time encoding interval. Therefore, spectrum $A(\nu)$ and its Fourier transform $I(x)$ are expressed in the following equation [16];

$$A(\nu) = F\{I(x)\} = \int_0^\infty I(x)\cos(2\pi\nu x)\,dx \qquad (3)$$

The second derivative is given by [17];

$$\frac{d^2A(\nu)}{d\nu^2} = F\{I(x)\} = \int_0^\infty (-2\pi x)^2 I(x)\cos(2\pi\nu x)\,dx \qquad (4)$$

The second derivative of band spectrum A^{II} becomes;

$$A^{II} = \frac{d^2A(\nu)}{d\nu^2} = -\frac{1}{\pi\gamma^2}\frac{2a(1-3a\nu^2)}{(1+a\nu^2)^{-3}}$$

Where a equals $1/\gamma^2$. However, the original peak frequency is identical to the peak frequency of the second derivative. The half-width of the original peak is related to the half-width of second derivative as $\frac{\gamma}{\gamma^{II}} = 2.7$ and also the peak intensity of the second derivative is related to the original intensity by ${A_0}^{II} = -2A_0/\gamma^2$ [12,13].

4. Statistics analysis

The significance level of the five groups was determined by one-way ANOVA. Followed by a post hoc test to examine the paired significance by using Origin 8 software. the value of $p < 0.05$ was accepted as a statistical significance.

5. Results and discussions.

The FTIR spectra of Hb in the range ~4000–400 cm^{-1} for both control and irradiated samples at different exposure time (5, 10, 20, 30 min) are shown in Fig 1. The figure also shows the contributions of the functional group peaks in all Hb samples.

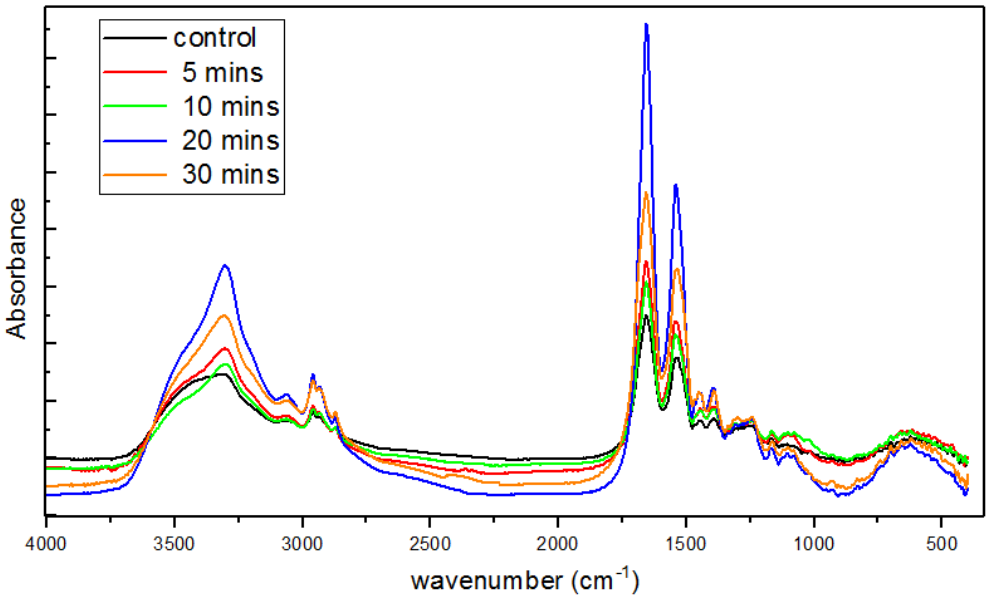

Figure 2. FTIR spectra of control and irradiated Hb samples.

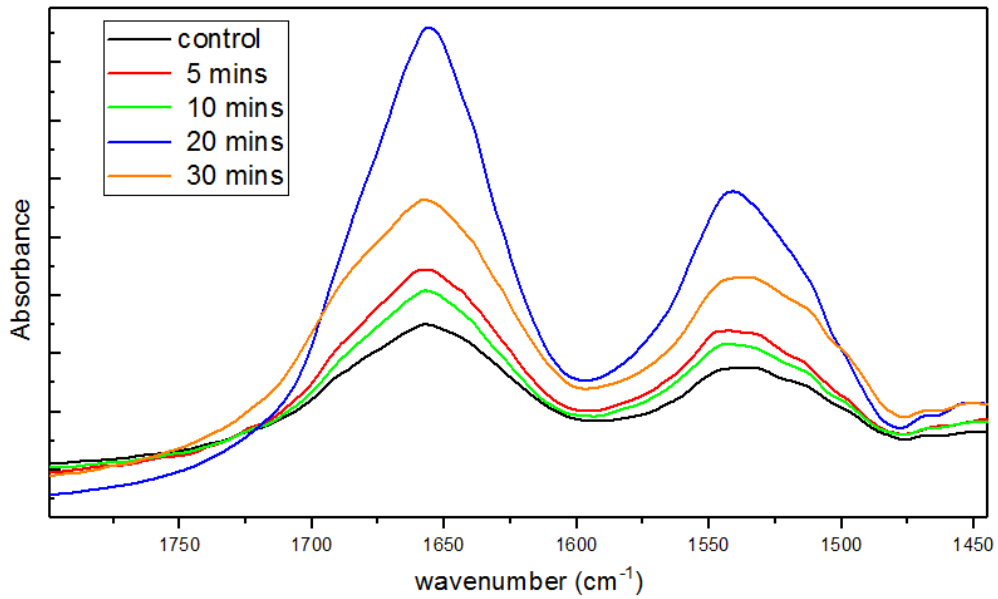

Figure 1. Spectra of amid I and amid II of all Hb samples

As shown in Fig1., all peaks are located at the same positions as well as there is no obvious change in the number of the essence bands for the

studied samples. However, there is a change in the intensities of the peaks might be attributed to the variation in the concentrations of samples in KBr pellets. The spectra of Amide I and II bands and at 1658 cm^{-1} and 1542 cm^{-1}, respectively are shown in Fig 2. The broad Amid I peak that located at 1700–1600 cm^{-1} can be formed by the superimposition of the conformational structures of proteins, such as alpha-helices, β-sheets, β-turns, and random coils [17], therefore it was selected for further analysis.

The spectra of the second derivative were obtained and smoothed using an eleven point Stavisky–Golay function with the help of Origin 8 software as shown in Fig 3. The smoothing process is carried out in order to minimize the distortion to amide I band components.

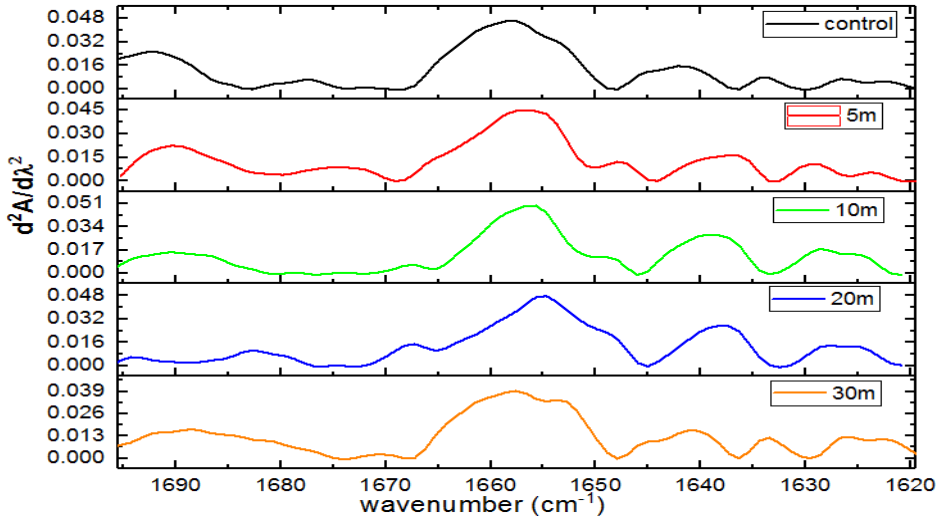

Figure 3. Secondary derivative mean FTIR spectra of all Hb samples.

As presented in Fig 3., the bands in the range (1654-1658 cm^{-1}) could be attributed to the α-helix of human haemoglobin [22]. β-sheets Bands was recognized in the regions of 1640−1620 cm^{-1} and 1699−1689 cm^{-1} [22–24]. The unordered conformation (usually named random coil) was located at 1644±3 cm^{-1}[18,22]. After baseline correction, the obtained smoothed second-derivative bands where curve fitted using Gaussian, Lorentzian, or a mixture of Gaussian/Lorentzian-shaped fitting for the control and irradiated samples at different exposure time (5, 10, 20, 30 min) to solve the spectrum of proteins into its major secondary structure components as shown in Figs 4,5,6,7 and 8. The process was mainly governed by the different characteristic band position, width, and position of the baseline. The relative areas of each band were used to determine each contribution of each secondary structure conformation.

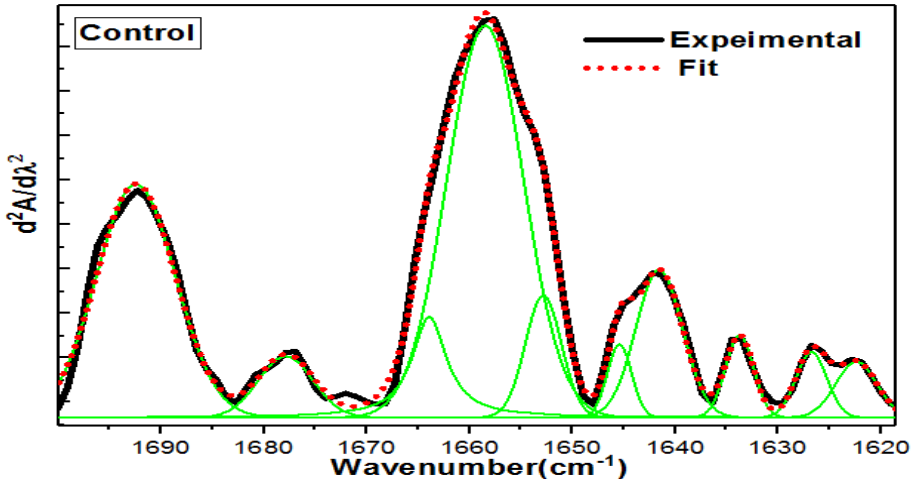

Figure 4. Curve fitting for the Second derivative spectra for the non-irradiated Hb sample.

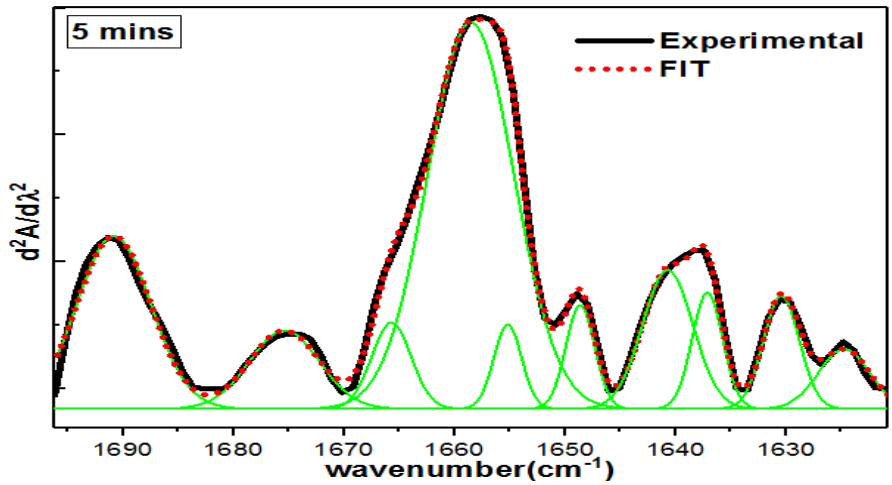

Figure 5. Curve fitting for the Second derivative for the 5 min irradiated Hb sample.

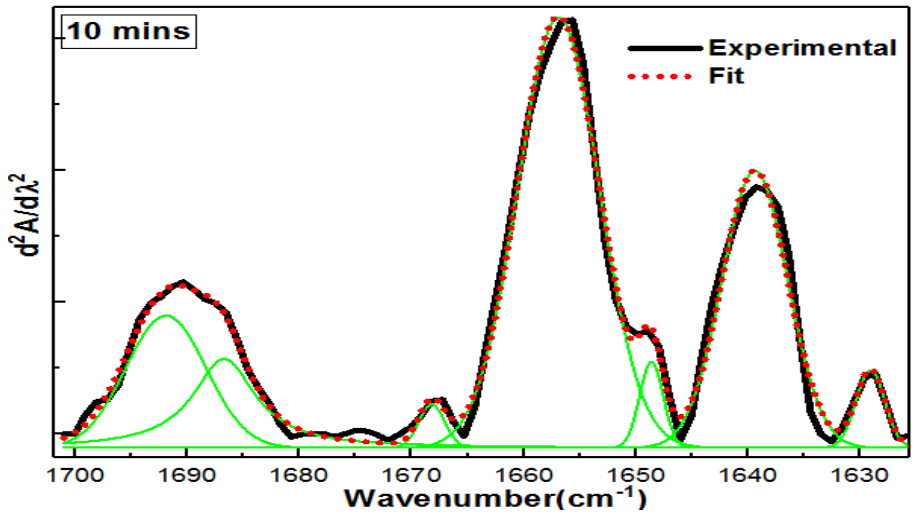

Figure 6. Curve fitting for the Second derivative for the 10 min irradiated Hb sample.

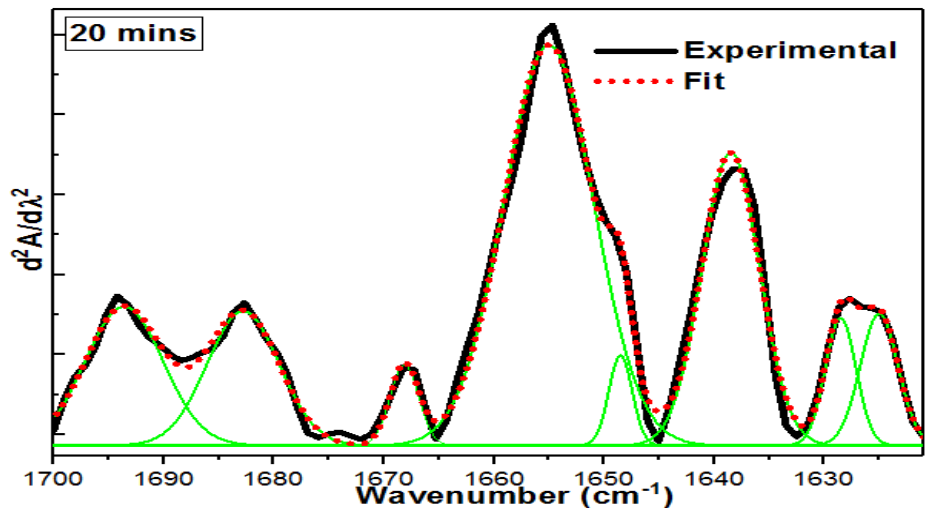

Figure 7. Curve fitting for the Second derivative for the 20 min irradiated Hb sample.

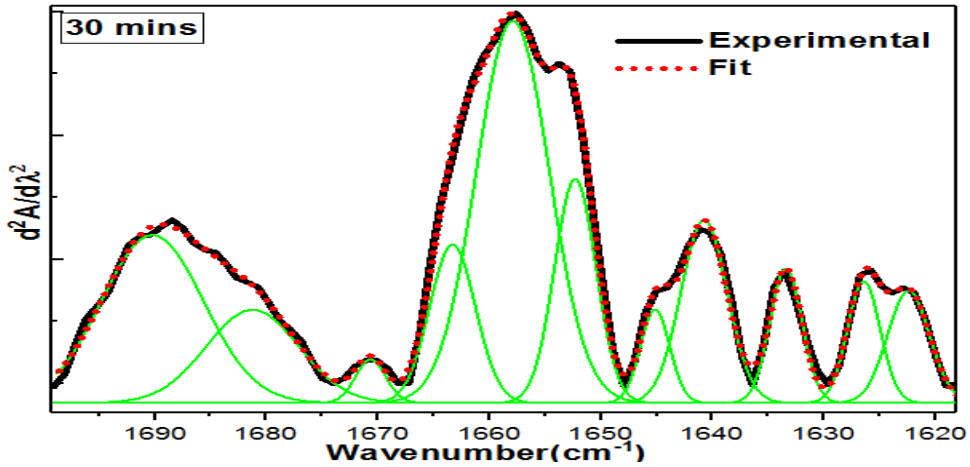

Figure 8. Curve fitting for the Second derivative for the 30 min irradiated Hb sample.

The contents ratio of the different secondary structure conformations according to Amide I band calculations are listed in table 2. All secondary structures components (α -helices, β -sheets, β -turns, and random coils) of the all Hb samples of the different irradiation duration groups were subjected to pairing comparisons. Comparing to the non-irradiated group (control), the 5, 10, and 20 min groups showed a slight change in the content of α -helix and random coil structures that did not reach statistical significance ($p > 0.05$). The 30 min group displayed a significant reduction in the content of α -helix accompanied by a significant increase in the random coil and β-turn structures compared with the non-irradiated group ($p < 0.05$). This decrease in alpha-helix structure may be explained as a photo-inductive degradation of alpha-helix contents to the unordered structure of random coils and β-turns.

Table 2. The percentage of contents of different secondary structure contents based on the curve-fitting analysis of the Amide I band.

Secondary structure	Percentage of content (%)				
	control	5min	10min	20min	30min
α -helix	46.50±1.378	45.62±1.290	45.44±0.484	42.84±1.052	36.11±2.916
Random coil	19.21±2.051	16.80±0.979	22.42±1.556	19.98±1.792	26.49±1.485
β -sheet	32.05±1.058	28.75±2.153	16.56±1.342	22.28±1.069	28.049±2.634
β -turns	2.22±1.238	8.81±0.994	15.57±3.195	14.88±0.58203	9.26±1.4951

Our results matched with the previous studies which proposed the formation of small amount of Reactive oxygen species (ROS) as a result of interaction between low-level laser and living systems such as erythrocytes. The ROS are produced in this case due to the photosensitization of cell chromophores such as heme-proteins [25–28]. Hemoglobin as a major chromophore in the blood can serve as a natural porphyrin substance and cause the ROS production when irradiated with low power laser at 630 nm [29]. The photodamage induced by low-level laser to blood is supposed to be relatively minimal compared to other body tissues because of the high absorption coefficient of haemoglobin [30,31]. A large amount of ROS can be produced at high energy irradiations which may lead to oxidative stress of the cell [32]. Another study revealed that low-level laser irradiation can induce photo-damage to the cells after long expoture time (more than 10 minutes)even at power values lower than 10 mW [33]. The present study supports the hypothesis that the ability of the laser light to induce phot-damage of alpha-helix structures of hemoglobin may be linked to the production of ROS.

6. Conclusion

The impact of low power laser on the secondary structure of all haemoglobin samples is well investigated. The secondary structure of irradiated and non-irradiated human hemoglobin was obtained by using FTIR spectra followed by the mathematical analysis of band-narrowing techniques. It was found no significant change in the content of alpha-helix structures at the groups of 5,10,20 minutes of irradiation. However, at 30 minutes group, there was a significant reduction of alpha-helix structures accompanied by a significant increase in the random coil and β-turn structure which may be explained as a photo-induced degradation of alpha-helix contents to the unordered structure of random coils and β-turns. We conclude that careful care and extra precisions have to be taken while the clinical application that includes the intravenous laser irradiation of blood to avoid the protein photodamage caused by the low power laser at long expoture time.

REFERENCES

[1] TH. M ,Stimulated Optical Radiation in Ruby, *Nature*, 1960 , **4736**

[2] Hamblin M R and Demidova T N 2006 Mechanisms of low level light therapy *Mech. Low-Light Ther.* **6140** 614001

[3] Lin F, Josephs S F, Alexandrescu D T, Ramos F, Bogin V, Gammill V, Dasanu C A, De Necochea-Campion R, Patel A N, Carrier E and Koos D R 2010 Lasers, stem cells, and COPD *J. Transl. Med.* **8** 1–10

[4] E Mester, B Szende P G 1968 The effect of laser beams on the growth of hair in mice *Radiobiol Radiother (Berl)* **9(5):621-6**

[5] Huang Y Y, Chen A C H, Carroll J D and Hamblin M R 2009 Biphasic dose response in low level lightherapy *Dose-Response* **7** 358–83

[6] Sutherland J C 2002 Biological Effects of Polychromatic Light *Photochem. Photobiol.* **76** 164

[7] Karu T I, Pyatibrat L V., Kolyakov S F and Afanasyeva N I 2008 Absorption measurements of cell monolayers relevant to mechanisms of laser phototherapy: Reduction or oxidation of cytochrome c oxidase under laser radiation at 632.8 nm *Photomed. Laser Surg.* **26** 593–9

[8] T. Lundeberg M M 1991 Low-Power HeNe laser Treatment of Venous leg Ulcers *Ann. Plast. Surg.* **27**

[9] Halevy, Sima R lubart 1997 Infrared (780) lOW LEVEL LASER THERAPY FOR WOUND HEALING *lASER Ther.*

[10] Farivar S, Malekshahabi T and Shiari R 2014 Biological effects of low level laser therapy *J. Lasers Med. Sci.* **5** 58–62

[11] Chung H, Dai T, Sharma S K, Huang Y Y, Carroll J D and Hamblin M R 2012 The nuts and bolts of low-level laser (Light) therapy *Ann. Biomed. Eng.* **40** 516–33

[12] Kujawa J, Pasternak K, Zavodnik I, Irzmański R, Wróbel D and Bryszewska M 2014 The effect of near-infrared MLS laser radiation on cell membrane structure and radical generation *Lasers Med. Sci.* **29** 1663–8

[13] Mi X Q, Chen J Y and Zhou L W 2006 Effect of low power laser irradiation on disconnecting the membrane-attached hemoglobin from erythrocyte membrane *J. Photochem. Photobiol. B Biol.* **83** 146–50

[14] Ramser K, Logg K, Goksör M, Enger J, Käll M and Hanstorp D 2004 Resonance Raman spectroscopy of optically trapped functional erythrocytes *J. Biomed. Opt.* **9** 593

[15] Dasgupta R, Ahlawat S, Verma R S, Uppal A and Gupta P K 2010 Hemoglobin degradation in human erythrocytes with long-duration near-infrared laser exposure in Raman optical tweezers *J. Biomed. Opt.* **15** 055009

[16] Ramser K, Bjerneld E J, Fant C and Käll M 2003 Importance of substrate and photo-induced effects in Raman spectroscopy of single functional erythrocytes *J. Biomed. Opt.* **8** 173

[17] Ye S, Ruan P, Yong J, Shen H, Liao Z and Dong X 2016 The impact of the HbA1c level of type 2 diabetics on the structure of haemoglobin *Sci. Rep.* **6** 1–8

[18] Yang H, Yang S, Kong J, Dong A and Yu S 2015 Obtaining information about protein secondary structures in aqueous solution using Fourier transform IR spectroscopy *Nat. Protoc.* **10** 382–96

[19] Cameron, David G. D J M 1987 A Generalized Approach to Derivative Spectroscopy *Appl. Spectrosc.* **41**

[20] Heino Susi and, Michael D 1983 PROTEIN STRUCTURE BY FOURIER TRANSFORM INFRARED SPECTROSCOPY: SECOND DERIVATIVE SPECTRA *Biochem. Biophys. Res. Commun.* **115** 391–7

[21] Kong J and Yu S 2007 Fourier transform infrared spectroscopic analysis of protein secondary structures *Acta Biochim. Biophys. Sin. (Shanghai).* **39** 549–59

[22] Dong A, Huang P and Caughey W S 1990 Protein Secondary Structures in Water from Second-Derivative Amide I Infrared Spectra *Biochemistry* **29** 3303–8

[23] Krimm B S and Bandekart J 1986 Vibrational spec and protein conformation

[24] Susi B H and Byler D M 1985 Resolution-Enhanced Fourier Transform Infrared Spectroscopy of Enzymes *Methods* **130** 290–311

[25] Zhang J, Xing D and Gao X 2008 Low-power laser irradiation activates Src tyrosine kinase through reactive oxygen species-mediated signaling pathway *J. Cell. Physiol.* **217** 518–28

[26] Paper O and Words K 2002 Biomedical Science Critical Role of Nlitochondrial Reactive Oxygen Species Formation in Visible Laser Irradiation-Induced Apoptosis in Rat Brain *J. Biomed. Sci.* **3283016** 507–16

[27] Godley B F, Shamsi F A, Liang F Q, Jarrett S G, Davies S and Boulton M 2005 Blue light induces mitochondrial DNA damage and free radical production in epithelial cells *J. Biol. Chem.* **280** 21061–6

[28] Zahra A-T 2014 Investigating the Effects of Green Laser Irradiation on Red Blood Cells: Green Laser Blood Therapy *Int. J. Appl. Res. Stud.* **3** 1–5

[29] Stadler I, Evans R, Kolb B, Naim J O, Narayan V, Buehner N and Lanzafame R J 2000 In vitro effects of low-level laser irradiation at 660 nm on peripheral blood lymphocytes *Lasers Surg. Med.* **27** 255–61

[30] Pfefer T J, Choi B, Vargas G, McNally K M and Welch A J 2000 Pulsed laser-induced thermal damage in whole blood *J. Biomech. Eng.* **122** 196–202

[31] Lapotko D O and Lukianova E Y 2005 Influence of physiological conditions on laser damage thresholds for blood, heart, and liver cells *Lasers Surg. Med.* **36** 13–21

[32] Dröge W 2002 Free radicals in the physiological control of cell function *Physiol. Rev.* **82** 47–95

[33] Barkur S, Bankapur A, Chidangil S and Mathur D 2017 Effect of infrared light on live blood cells: Role of β-carotene *J. Photochem. Photobiol. B Biol.* **171** 104–16